Computational study of the spin-forbidden H 2 oxidative addition to 16-electron Fe(0) complexes

Jeremy Harvey, Rinaldo Poli

Computational study of the spin-forbidden H_2 oxidative addition to 16-electron Fe(0) Complexes.

Jeremy N. Harvey[a] and Rinaldo Poli[b]

[a]*School of Chemistry, University of Bristol, Cantock's Close, Bristol BS8 1TS, U.K.*

[b]*Laboratoire de Synthèse et d'Electrosynthèse Organométalliques (LSEO UMR 5632), Université de Bourgogne, Faculté de Sciences "Gabriel", 6 boulevard Gabriel, 21000 Dijon, France.*

Proofs to:

R. Poli

+33-380396881

+33-380393720

poli@u-bourgogne.fr

Abstract

The spin-forbidden oxidative addition of H_2 to $Fe(CO)_4$, $Fe(PH_3)_4$, $Fe(dpe)_2$ and $Fe(dmpe)_2$ [dpe = $H_2PCH_2CH_2PH_2$, dmpe = $(CH_3)_2PCH_2CH_2P(CH_3)_2$] has been investigated by density functional theory using a modified B3PW91 functional. All 16-electron fragments are found to adopt a spin triplet ground state. The H_2 addition involves a spin crossover in the reagents region of configurational space, at a significantly higher energy relative to the triplet dissociation asymptote and, for the case of $Fe(CO_4)$•H_2, even higher than the singlet dissociation asymptote. After crossing to the singlet surface, the addition proceeds directly to the classical *cis*-dihydride product. Only for the $Fe(CO)_4$ was it possible to locate a stable energy minimum for the nonclassical tautomer (dihydrogen complex), but the energy difference between this minimum and the tautomerisation transition state inverts when taking into account the zero point energy correction. The geometries at the crossing points indicate a "side-on" approach of the H_2 molecule to the metal for the $Fe(CO)_4$, $Fe(CO)_2(PH_3)_2$, and $Fe(PH_3)_4$ systems. These geometries are more reactants-like for the $Fe(CO)_4$ system and more product-like for the $Fe(PH_3)_4$ system. The crossing point geometry for the $Fe(dpe)_2$ system, on the other hand, is nearly C_2-symmetric. The presence of an energy barrier on going from $^3FeL_4+H_2$ to the crossing point is in agreement with the slow observed rates for addition of H_2 to these unsaturated organometallic fragments.

Introduction

It has recently been shown that thermal reactions implicating more than one spin surface are common in different areas of transition metal chemistry, including oxo-transfer, C-H activation, metal-catalysed polymerisation, and bioinorganic chemistry.[1-5] Besides the obvious situations where reactants and products have different spin, it is also possible that reagents in a particular spin state are transformed into products of the same spin, via one or more intermediates of different spin and an even number of spin crossovers. This event was shown to have profound effects on reaction rates[6] and on product distributions.[7] In many cases, however, the very short lifetime of the intermediates does not allow their direct identification by experimental method. The correct interpretation of reaction rates and mechanisms, therefore, requires the explicit computation of the point in configuration space at which the system crosses from one spin surface to another. This is the point at minimum energy within the seam of crossing between the two surfaces, or Minimum Energy Crossing Point (MECP).[8-12] The ability to locate and characterise MECPs between potential energy surfaces of different spin for realistic transition-metal containing systems, first demonstrated in ref. 6, is key to understanding spin-forbidden reactions.[13]

Among organometallic reaction intermediates, $Fe(CO)_4$ has attracted considerable attention. Its ground state triplet is now solidly established both at the experimental[14-22] and theoretical levels.[23-33] The experimental observation that the spin forbidden CO addition to yield singlet $Fe(CO)_5$ is ca 400 times slower than the spin-allowed addition to $Fe(CO)_3$ has prompted the proposition[15] that this extra barrier is related to the need to achieve a suitable geometry for the spin crossing to occur, *i.e.* the need to reach a MECP. The explicit calculation of the MECP for this reaction has only recently been carried out [33] and a good agreement was obtained between the computed and the experimental activation barriers, in

support of the mechanistic proposition. This observation is relevant because the spin-forbidden CO additions to other 16-electron triplet complexes have been shown to be limited by a normal steric barrier while the crossing point resides on the down slope leading to the product.[34, 35]

The oxidative addition of dihydrogen to unsaturated transition metal complexes is another reaction of fundamental importance to organometallic chemistry and homogeneous catalysis. The H_2 oxidative addition to $Fe(CO)_4$ has been investigated experimentally[16] and theoretically.[28] The experimental study has shown that the reaction rate is three orders of magnitude slower than the H_2 addition to related electronically unsaturated complexes, a phenomenon tentatively attributed to the spin forbidden character of the process. The theoretical study, however, did not include the explicit calculation of the MECP. A related process is the H_2 oxidative addition to $M(dmpe)_2$ (M = Fe and Ru; dmpe = $Me_2PCH_2CH_2PMe_2$).[36, 37] Interestingly, the rate constant for H_2 addition is 7500 times smaller for $Fe(dmpe)_2$ than for $Ru(dmpe)_2$, whereas the CO addition is diffusion-controlled for both complexes. A theoretical study on model $M(PH_3)_4$ (M = Fe, Ru) compounds shows that the Ru species adopts a singlet ground state, whereas the Fe species adopts a triplet ground state. The study, however, did not include a thorough analysis of the spin crossover region.[38]

In this contribution, we intend to examine in more detail (*i.e.* including the explicit MECP computation) the reaction coordinate for the spin-forbidden H_2 oxidative addition to the already investigated $Fe(CO)_4$ and $Fe(PH_3)_4$ systems, and to extend the study to the mixed-ligand $Fe(CO)_2(PH_3)_2$ system, to the less approximate $Fe(dpe)_2$ model (dpe = $PH_2CH_2CH_2PH_2$) of the real $Fe(dmpe)_2$ complex, as well as to the real complex itself.

Results and Discussion

Singlet and triplet 16-electron Fe(0) complexes

When studying chemical reactivity, it is essential to use a computational method which is as accurate as possible, and this can be very hard to achieve in transition metal chemistry given the delicate balance of exchange and correlation effects, the frequently poor performance of the simplest correlated *ab initio* methods such as MP2, and the need for very large basis sets. By and large, density functional theory (DFT) has been found to give very good results in the study of inorganic and organometallic systems. However, in a previous study, [33] different density functionals were found to predict very different energetic properties for the $Fe(CO)_4$ + CO system, both for the spin-state splitting between triplet and singlet $Fe(CO)_4$, and for the bond energy. After extensive calibration using accurate *ab initio* methods (CCSD(T) with large basis sets), it was concluded that the best description of this system is obtained using a modified form of the hybrid B3PW91 functional. This new functional, referred to as B3PW91*, is identical to B3PW91 except that the coefficient c_3 describing the mixing of "exact", Hartree-Fock, exchange is reduced to 0.15 (vs. 0.20 in B3PW91). This reduced mixing of exact exchange has been found by others to give better agreement for spin-state splittings in other iron compounds.[39] In our present calculations, we have used this B3PW91* functional throughout, together with the same type of flexible, polarised basis set also used in ref. [33], so that the results should be directly comparable.

As well as considering anew the potential energy surfaces for addition of H_2 to $Fe(CO)_4$, our calculations were extended to derivatives containing two CO and two PH_3 ligands, and to others containing four P-donor ligands. All systems investigated, and relevant bond distances and angles, are shown in Figure 1. The $Fe(CO)_2(PH_3)_2$ system can exist as three possible isomers, identified as **A**, **B** and **C** in Figure 1. Among these, only isomer **A** gave a stable

minimum in both spin states. Isomer **B** only gave a triplet minimum, while isomer **C** only gave a singlet minimum. Singlet **B** reverted to singlet **A** during the optimisation, whereas triplet **C** reverted to triplet **A**. The most stable isomer is **A** for both spin states.

All 16-electron Fe(0) complexes were found to adopt a triplet ground state, the triplet-singlet gap being higher for the tetrakis(phosphine) complexes, intermediate for the bis(phosphine)dicarbonyl complex, and lowest for the tetracarbonyl complex. This trend agrees with that obtained at the BP86 level by Macgregor *et al.*[38]on going from $Fe(CO)_4$ to $Fe(PH_3)_4$. Amongst the phosphine derivatives, the triplet-singlet gap varies in the order $Fe(PH_3)_4$ > $Fe(dpe)_2$ > $Fe(dmpe)_2$, so that the dpe complex is a better model than the PH_3 complex for the real dmpe system. Alkyl substitution makes dpe and especially dmpe a better σ-donor, as confirmed by the greater negative Mulliken charge in the order $Fe(PH_3)_4$ < $Fe(dpe)_2$ < $Fe(dmpe)_2$, for both spin states. The consequent stronger donating power in the dpe and dmpe complexes is consistent with the lower triplet-singlet energy gap.

The geometries are essentially identical in their gross features for all systems. Both the L_{ax}-Fe-L_{ax} and L_{eq}-Fe-L_{eq} angles are wider for the singlet geometries relative to the corresponding triplets, whereas all bond distances are slightly shorter in the singlet structures. The distance to any given ligand is systematically longer when this is located in the axial position, no matter the spin state. The distances obtained for $Fe(PH_3)_4$ are only marginally but systematically longer than those obtained for the same molecule at the BP86 level,[38] for both spin states. For singlet $Fe(CO)_4$, whose geometry has recently been determined experimentally by ultrafast electron diffraction methods, the optimized geometry is in excellent agreement with the experiment (Fe-C_{ax} = 1.81(3) Å; Fe-C_{eq} = 1.77(3) Å; C_{ax}-Fe-C_{ax} = 169(2)°; C_{eq}-Fe-C_{eq} = 125(3)°)[22]. Substitution effects give the expected trends. Thus, replacement of two CO ligands with as many PH_3 ligands leads to a Fe-C bond shortening for the two residual CO ligands in $Fe(CO)_2(PH_3)_2$ (independently on the spin state and

stereochemistry), a phenomenon attributable to the increase of Fe-CO π back-bonding. Analogously, the further replacement of the two residual CO ligands, leading to $Fe(PH_3)_4$, is accompanied by a Fe-PH_3 bond shortening, again independently on the spin state and stereochemistry. This effect may be attributed to an analogous increase of Fe-PH_3 π back-bonding. The effect of changing the nature of the phosphorus donor on going from $Fe(PH_3)_4$ through $Fe(dpe)_2$ to $Fe(dmpe)_2$ is only marginal on the Fe-P bond lengths.

<Insert Figure 1 here>

Products of H_2 addition to the 16-electron Fe(0) complexes.

The addition of H_2 to the above mentioned 16-electron Fe(0) species ultimately affords dihydride products. The energy gains associated to the oxidative addition processes are shown in Table 1 for all systems. Relative to the 16-electron singlet precursor, the exothermicity increases as the number of P-donor ligands increases. This correlates with the better ability of the P-donor ligands to stabilise the formally higher oxidation state. For the mixed CO-PH_3 system, the most stable oxidative addition product is again derived from isomer **A**. The energy of the other isomers increases as the σ-donating power of the ligands *trans* to H increases (CO < PH_3 << H), in agreement with well know arguments of σ competition and *trans* labilisation.[40, 41] Therefore, all further investigations along the H_2 oxidative addition co-ordinate (see next section) were carried out on this isomer only. The dpe model is worse than the PH_3 model for the dmpe complex in terms of reproducing the energy gain of the H_2 oxidative addition from the singlet state. Both models are equally inappropriate, on the other hand, for what concerns the energy gain from the triplet state. The only experimental data available to compare our results with concerns the tetracarbonyl series. From the activation energies for H_2 dissociation from $Fe(CO)_4(H)_2$ and for H_2 addition to

triplet $Fe(CO)_4$, ΔH for dissociation was determined to be 88 ± 8 kJ mol^{-1}.[16] Our computed value of ΔH, 89.5 kJ mol^{-1} is in excellent agreement with this value. Previous calculations[28] at the BP86 level also gave good agreement for ΔH, but with a very low singlet/triplet energy splitting, whereas the B3LYP and BLYP functionals gave a poor ΔH. These observations are consistent with our survey of many different functionals[33] and confirm our impression that B3PW91* gives accurate results for these iron-containing systems.

<Insert Table 1 here>

Only in the case of $Fe(CO)_4$ was it possible to identify an intermediate dihydrogen complex as a stable local minimum. This is 27.1 kJ mol^{-1} less stable than the dihydride product (*cf.* 25.9 kJ mol^{-1} at the BP86 level).[28] Its geometry and selected parameters are shown in Figure 2, together with those of all classical dihydride products. The transition state (TS) between the nonclassical and classical products has also been optimised. The nature of the resulting geometry as a first order saddle point is confirmed by the frequency analysis, which shows a single imaginary frequency corresponding to the H_2 stretch, see Table 1. Its energy is only slightly higher than the nonclassical minimum (1.2 kJ mol^{-1}, *cf.* 1.7 kJ mol^{-1} at the BP86 level[28]), in agreement with a very facile conversion to the final product. Thus, there is good agreement between the results obtained with the BP86 and B3PW91* functionals. However, we note that the energy difference between the nonclassical isomer and the TS is reversed upon adding the zero-point energy correction and further addition of the thermal and entropy contributions maintains this reversal. This would seem to suggest that this nonclassical isomer is probably not a true intermediate in the H_2 oxidative addition process.

For the $Fe(PH_3)_4$ and $Fe(dpe)_2$ systems, partial geometry optimisations were carried out with a frozen $Fe(H_2)$ unit, keeping the Fe-H and H-Fe-H parameters fixed at the values found

for the $Fe(CO)_4(H_2)$ complex. The resulting structures, which were 56.1 and 44.4 kJ mol^{-1} higher in energy than the corresponding dihydride products, were then further refined freely and collapsed back to the dihydride products. Given the greater donor ability of phosphine ligands relative to CO and the doubtful intermediacy of the nonclassical isomer even for the tetracarbonyl system (*vide supra*), this is not an unexpected result. In fact, using Hammond's postulate arguments, it is easy to accept that the greater exothermicity of the insertion for the mixed CO-PH_3 and for the all-phosphine systems would make the small barrier to insertion present in the $Fe(CO)_4$ system completely disappear.

The structures of the products obtained from $Fe(CO)_4$ have already been extensively discussed previously.[28] In particular, the calculations reproduced the experimental preference for a *cis*-dihydride structure relative to the *trans* isomer. Therefore, we did not consider the *trans* structure in our calculations. Relative to that study, which used the BP86, BLYP and B3LYP functionals, all distances are slightly shorter and angles are approximately identical. All these parameters are quite close to those experimentally determined for *cis*-$FeH_2(CO)_4$.[42] The geometry of the FeH_2 moiety is approximately identical in all dihydride products. On going from the singlet FeL_4 to the corresponding *cis*-FeH_2L_4 species, all Fe-L_{ax} bonds (*trans* to each other) shorten, a phenomenon which may be due to going from effective Fe(0) to Fe(II), whereas all Fe-L_{eq} bonds (*trans* to H ligands) lengthen, a phenomenon which can be attributed to the strong *trans*-influence of the hydride ligand. There appears to be only one structural determination for a *cis*-FeH_2L_4 complex having L = P-donor ligand, *i.e.* with L = $PPh(OEt)_2$.[43] An appropriate check of the computational accuracy is prevented by the high uncertainly on the Fe-H distance [1.50(5) Å], due to the determination by X-ray diffraction, and by the electronic difference between the phosphonite ligands [Fe-P_{ax} = 2.128(7) Å; P_{eq} = 2.149(3) Å] and the phosphines used in our models. There is a rather good agreement, however, between the computed values and those observed in this structure. Other related structurally

characterised compounds, *e.g.* $FeH_2(dppm)_2$,[44] $FeH_2(dppe)_2$[45] and $FeH(HBH_3)(dppe)_2$,[46] adopt the alternative *trans* geometry.

The computed Fe-H stretching frequencies follow a clear trend, being lower when the co-ordination sphere is more donating/less π-accepting [*e.g.* $Fe(CO)_4H_2$ >> $Fe(PH_3)_4H_2$ > $Fe(dpe)_2H_2$ > $Fe(dmpe)_2H_2$]. This trend cannot be attributed to π competition effects, since the Fe-H bonds do not have a π bonding component. A similar trend has been noted previously for hydride ligand when the metal is oxidised and the reasons for this trend have been critically discussed.[47] For instance, the Fe-H stretching vibrations in a series of Fe(II) complex Cp*FeH(LL) are found at lower frequencies than the corresponding vibrations in the related Fe(III) complexes $[Cp^*FeH(LL)]^+$.[48, 49] and the same trend is observed for $[Cp^*WH_3(dppe)]^{n+}$ on going from n = 0 to n = 1.[50] We can therefore associate the computed trend of Fe-H stretching frequencies in compounds $Fe(L)_4H_2$ to a similar tuning of the metal electron density by the nature of the ancillary ligands. For the series of $Fe(CO)_2(PH_3)_4H_2$ isomers, the frequencies clearly respond to the influence of the *trans* ligands and correlate with the Fe-H distances.

<Insert Figure 2 here>

Minimum Energy Crossing Points.

To study the reactivity in these systems, it is of course also necessary to locate the critical point for H_2 addition to the triplet reactant. In all the systems studied here, this is the MECP between the triplet and singlet surfaces in the reactant region of both potential energy surfaces. At first sight, it may appear inadequate to consider only the energetics of the MECP. In the language of transition state theory, the need to cross from one surface to another adds an extra "transmission factor", usually smaller than one, to the overall rate coefficient. This explains why two reactions with an identical MECP energy, but with much stronger spin-orbit

coupling in one case than in the other, will occur at different rates. However, non-adiabatic versions of transition state theory show that the transmission factor only varies quadratically with the strength of spin-orbit coupling.[51] Furthermore, spin-orbit coupling constants between the singlet and triplet wavefunctions are probably rather similar at all the MECPs discussed here. In contrast, the MECP energies described here are significantly different from system to system, and the rate coefficient varies exponentially with MECP energy.[51] To an excellent first approximation, therefore, we focus on the energetics of the MECPs only in this work.

We have located the MECP for approach of dihydrogen to $Fe(CO)_4$, to isomer A of $Fe(CO)_2(PH_3)_2$, and to the all-phosphine systems $Fe(PH_3)_4$ and $Fe(dpe)_2$, and the optimised structures are shown in Fig. 3, with the corresponding energetics in Table 1 and in Figure 4. In the carbonyl, mixed CO/PH_3 and PH_3 systems, the optimized MECP has the incoming H_2 molecule lying "side-on" to the metal, in the plane formed by the two "equatorial" ligands, and roughly *trans* to one of them. In other words, H_2 does *not* approach along the C_2 axis of symmetry of the unsaturated fragment, which would be the least-motion pathway for addition to the singlet. The approach of H_2 from the "side" of the $Fe(L)_4$ moiety is similar to the MECP structure found for the CO + $Fe(CO)_4$ system, where this mode of approach was found to give rise to a lower energy MECP as compared to approach along the C_2 axis.[33] This preference for not approaching along the C_2 axis may be due to the fact that in the triplet state, the a_1 singly-occupied orbital in $^3Fe(CO)_4$ has some 4s character and is more repulsive at longer range than the other, b_1 symmetric singly-occupied orbital, which does not have any 4s character. The MECP for the $Fe(dpe)_2$ system is the "latest" and most product-like, and this may explain why it adopts C_2 symmetry, as the singlet state is more attractive with this type of approach, especially at short M-H distances.

<Insert Figures 3 and 4 here>

In a simple one-dimensional model, the geometry of the crossing point between the repulsive triplet and attractive singlet states would be correlated with the singlet-triplet energy gap of the fragment $M(L)_4$. For the tetracarbonyl, mixed CO/PH_3 and tetra-PH_3 systems, for which the triplet-singlet energy splitting increases in this order, this expected correlation is indeed observed, as can be seen in Figure 3: the $Fe(CO)_4•H_2$ MECP is "earliest", with r(Fe–H) = ca. 2.2 Å, whereas the other two systems have r(Fe–H) = ca. 2.0 and 1.8 Å, respectively. For the $Fe(dpe)_2$ system, however, the correlation breaks down, since this has a smaller singlet-triplet gap than the $Fe(PH_3)_4$ system, yet the MECP is as noted previously the "latest" of all those systems studied, with r(Fe–H) = 1.71 Å, and a symmetric, C_2, H_2 bonding geometry as in the final adduct. This is probably due to the fact that as noted previously (see e.g. ref. [6]) the one-dimensional model for crossing is inadequate: *all* the geometric coordinates need to be the same at the MECP, whereas the geometries of the metallic fragment in its two spin states are not the same. In the present case, the geometry of the MECP is determined not only by the singlet-triplet gap, the degree of Fe–H_2 repulsion in the triplet and of attraction in the singlet, but also by issues relating to the extent to which the structure of the singlet and the triplet need to distort so as to reach a common geometry. Clearly, the latter factor must explain why the $Fe(dpe)_2•H_2$ is "later" than the $Fe(PH_3)_4•H_2$ one, despite the larger energy splitting in the latter. Related to this issue, it is also interesting to note that the internal geometry of the FeL_4 core in the MECP geometries is closer to the free *triplet* FeL_4 molecule for the first three systems, and closer to the free *singlet* FeL_4 molecule for the dpe system (*cf.* Figure 1 and Figure 3).

The *energy* for the MECPs is also of interest. As can be seen in Figure 4, all of the MECPs lie higher in energy than the corresponding $^3FeL_4 + H_2$ dissociation asympote. In fact, the $^{1,3}Fe(CO)_4•H_2$ MECP even lies higher in energy than the *singlet* dissociation asymptote,

and the MECP in the $Fe(CO)_2(PH_3)_2$ is very close in energy to the singlet asymptote. This situation is impossible to explain in the one-dimensional picture, given that the $^1Fe(CO)_4 – H_2$ interaction is almost purely attractive, but this is again due to the need to bring both fragments to a common geometry. The relatively high energy of the MECPs in all cases suggests that the rate of addition of H_2 to unsaturated fragments FeL_4 should proceed significantly slower than the collisional or diffusion rate, and this has indeed been observed experimentally. Gas-phase addition to $Fe(CO)_4$ (under high-pressure limiting conditions)[16] is ca. 3 orders of magnitude smaller than is typical for addition of H_2 to other coordinatively unsaturated species, and $Fe(dmpe)_2$ reacts with dihydrogen roughly 7500 times slower than does $Ru(dmpe)_2$[36, 37] – the reaction in the latter case involves only singlet states and, based on calculations carried out for the $Ru(PH_3)_4$ model, does not involve an energy barrier. In this sense, our predictions are in very good agreement with experiment: the slow observed rates for addition of H_2 to these unsaturated organometallic fragments are due to the existence of a barrier on the adiabatic potential energy surface, due to the need to cross from one spin state to another. In previous work, we have shown that the height of such barriers can be related to reactivity for CO addition to $Fe(CO)_4$[33] and for CO and N_2 addition to $Cp^*Mo(Cl)(PMe_3)_2$.[34, 35] In future work, we plan to use a non-adiabatic version of transition-state theory[33] to evaluate whether our calculated barrier heights lead to correct prediction of rates for addition of H_2 and other small molecules to $Fe(CO)_4$ and $Fe(dmpe)_2$. At present, it appears that the fairly large energy barriers required to reach the MECPs may lead to predicted rates which are too low, which suggests that further refinement of the level of theory may be necessary to achieve quantitative accuracy.

Conclusions

The present computational investigation explores for the first time the details of the spin crossing region for the H_2 oxidative addition to a spin triplet 16-electron fragment. The approach of the H_2 molecule, a weak ligand, to spin triplet FeL_4 is initially repulsive and necessitates significant molecular rearrangement before reaching the crossover region, leading to a significant energy barrier for the reaction. This situation is analogous to that observed for the oxidative addition of C-H bonds to spin triplet $CpIr(PH_3)$[7] and to Cp_2W, Cp^*_2W and $CH_2(C_5H_4)_2W$,[52] whereas the addition of stronger ligands such as CO may occur without the presence of a spin crossover barrier.[1, 2]

Computational Details

All calculations were carried out using the Gaussian 98 program code,[53] together with a modified form of the B3PW91 functional, and flexible polarized basis sets. Specifically, the c_3 coefficient in Becke's original three-parameter fit to thermochemical data[54] was changed to 0.15, to give the "B3PW91*" functional. For Fe, C and O and P, the triple-zeta basis sets of Schäfer *et al.*[55] were used. These basis sets were augmented with two diffuse, 4*p*-like functions (α = 0.134915 and 0.041843)[56] and an *f* polarisation function (α = 1.) on iron; and by one *d* polarisation function on C, O and P (α = 0.8, 1.2 and 0.55, respectively). The hydrogen atoms of the incoming H_2 molecule also used the triple-zeta basis,[55] with one *p* polarisation function (α = 0.75), whereas the hydrogen atoms on the phosphine ligands were treated with a split-valence basis set.[55] All minima and transition states were fully optimised and characterised by computing vibrational frequencies at the same level of theory. MECPs were optimised using the code developed by one of the authors[12] together with Gaussian98.[53] The MECP optimisation procedure is based on minimising a generalised gradient found at any geometry by combining the computed energies and gradients at that point on the two

potential energy surfaces. The gradient contains one term pointing towards the hyperspace in which the two surfaces intesect, and one term pointing towards lower energies within this hypersurface. The mixed Fortran/sheel script code (ref. 12, this program is available upon request) creates Gaussian input files for both spin states at a given geometry, calls Gaussian, extracts energies and gradients from the output files, tests for convergence, and cycles.

Acknowledgment

RP thanks the Conseil Régional de Bourgogne for funding to upgrade the laboratory's computing facility and CINES for a grant of free CPU time.

Supporting Information

Cartesian coordinates for all optimized geometries (4 pages).

References

1 R. Poli and J. N. Harvey, *Chem. Soc. Rev*, 2003, **32**, 1.
2 J. N. Harvey, R. Poli, and K. M. Smith, *Coord. Chem. Rev.*, in press.
3 S. Shaik, D. Danovich, A. Fiedler, D. Schröder, and H. Schwarz, *Helv. Chim. Acta*, 1995, **78**, 1393.
4 S. Shaik, M. Filatov, D. Schröder, and H. Schwarz, *Chem. Eur. J.*, 1998, **4**, 193.
5 D. Schröder, S. Shaik, and H. Schwarz, *Acc. Chem. Res.*, 2000, **33**, 139.
6 K. M. Smith, R. Poli, and J. N. Harvey, *New J. Chem.*, 2000, **24**, 77.
7 K. M. Smith, R. Poli, and J. N. Harvey, *Chem. Eur. J.*, 2001, **7**, 1679.
8 N. Koga and K. Morokuma, *Chem. Phys. Lett.*, 1985, **119**, 371.
9 A. Farazdel and M. Dupuis, *J. Comput. Chem.*, 1991, **12**, 276.
10 D. R. Yarkony, *J. Phys. Chem.*, 1993, **97**, 4407.
11 M. J. Bearpark, M. A. Robb, and H. B. Schlegel, *Chem. Phys. Lett.*, 1994, **223**, 269.
12 J. N. Harvey, M. Aschi, H. Schwarz, and W. Koch, *Theor. Chem. Acc.*, 1998, **99**, 95.
13 J. S. Hess, S. Leelasubcharoen, A. L. Rheingold, D. J. Doren, and K. H. Theopold, *J. Am. Chem. Soc.*, 2002, **124**, 2454.
14 M. Poliakoff and E. Weitz, *Acc. Chem. Res.*, 1987, **20**, 408.
15 R. J. Ryther and E. Weitz, *J. Phys. Chem.*, 1991, **95**, 9841.
16 W. Wang, A. A. Narducci, P. G. House, and E. Weitz, *J. Am. Chem. Soc.*, 1996, **118**, 8654.
17 L. Banares, T. Baumert, M. Bergt, B. Kiefer, and G. Gerber, *J. Chem. Phys.*, 1998, **108**, 5799.
18 O. Rubner, T. Baumert, M. Bergt, B. Kiefer, G. Gerber, and V. Engel, *Chem. Phys. Lett.*, 2000, **316**, 585.
19 O. Rubner and V. Engel, *Chem. Phys. Lett.*, 1998, **293**, 485.
20 M. Erdmann, O. Rubner, Z. Shen, and V. Engel, *Chem. Phys. Lett.*, 2001, **341**, 338.
21 P. T. Snee, C. K. Payne, S. D. Mebane, K. T. Kotz, and C. B. Harris, *J. Am. Chem. Soc.*, 2001, **123**, 6909.
22 H. Ihee, J. M. Cao, and A. H. Zewail, *Angew. Chem., Int. Ed. Engl.*, 2001, **40**, 1532.
23 L. A. Barnes, M. Rosi, and C. W. Bauschlicher, *J. Chem. Phys.*, 1991, **94**, 2031.
24 B. J. Persson, B. O. Roos, and K. Pierloot, *J. Chem. Phys.*, 1994, **101**, 6810.
25 B. Delley, M. Wrinn, and H. P. Luthi, *J. Chem. Phys.*, 1994, **100**, 5785.
26 A. W. Ehlers and G. Frenking, *Organometallics*, 1995, **14**, 423.
27 J. Li, G. Schreckenbach, and T. Ziegler, *J. Am. Chem. Soc.*, 1995, **117**, 486.
28 W. Wang and E. Weitz, *J. Phys. Chem. A*, 1997, **101**, 2358.
29 S. A. Decker and M. Klobukowski, *J. Am. Chem. Soc.*, 1998, **120**, 9342.
30 O. Rubner, V. Engel, M. R. Hachey, and C. Daniel, *Chem. Phys. Lett.*, 1999, **302**, 489.
31 O. GonzalezBlanco and V. Branchadell, *J. Chem. Phys.*, 1999, **110**, 778.
32 A. Ricca, *Chem. Phys. Lett.*, 2001, **350**, 313.
33 J. N. Harvey and M. Aschi, *Faraday Disc.*, 2003, **124**, in press.
34 D. W. Keogh and R. Poli, *J. Am. Chem. Soc.*, 1997, **119**, 2516.
35 V. R. Jensen and R. Poli, *J. Phys. Chem. A*, 2003, **107**.
36 C. Hall, W. D. Jones, R. J. Mawby, R. Osman, R. N. Perutz, and M. K. Whittlesey, *J. Am. Chem. Soc.*, 1992, **114**, 7425.
37 M. K. Whittlesey, R. J. Mawby, R. Osman, R. N. Perutz, L. D. Field, M. P. Wilkinson, and M. W. George, *J. Am. Chem. Soc.*, 1993, **115**, 8627.
38 S. A. Macgregor, O. Eisenstein, M. K. Whittlesey, and R. N. Perutz, *J. Chem. Soc., Dalton Trans.*, 1998, 291.

[39] O. Salomon, M. Reiher, and B. A. Hess, *J. Chem. Phys.*, 2002, **117**, 4729.

[40] A. Albinati, V. I. Bakhmutov, K. G. Caulton, E. Clot, J. Eckert, O. Eisenstein, D. G. Gusev, V. V. Grushin, B. E. Hauger, W. T. Klooster, T. F. Koetzle, R. K. McMullan, T. J. O'Laughlin, M. Pélissier, J. S. Ricci, M. P. Sigalas, and A. B. Vymenits, *J. Am. Chem. Soc.*, 1993, **115**, 7300.

[41] K. Abdur-Rashid, S. E. Clapham, A. Hadzovic, J. N. Harvey, A. J. Lough, and R. H. Morris, *J. Am. Chem. Soc.*, 2002, **124**, 15104.

[42] E. A. McNeill and F. R. Scholer, *J. Am. Chem. Soc.*, 1977, **99**, 6243.

[43] L. J. Guggenberger, H. B. Gray, D. D. Titus, R. E. Marsh, M. T. Flood, and A. A. Orio, *J. Am. Chem. Soc.*, 1972, **94**, 1135.

[44] Y. Gao, D. Holah, A. Hughes, G. Spivak, M. Havighurst, V. Magnuson, and V. Polyakov, *Polyhedron*, 1997, **16**, 2797.

[45] E. B. Lobkovskii, M. Y. Antipin, A. P. Borisov, V. D. Makhaev, K. N. Semenenko, and Y. T. Struchkov, *Koord. Khim.*, 1980, **6**, 1267.

[46] R. Bau, H. S. H. Yuan, M. V. Baker, and L. D. Field, *Inorg. Chim. Acta*, 1986, **114**, L 27.

[47] R. Poli, in 'Recent Advances in Hydride Chemistry', ed. R. Poli and M. Peruzzini, Amsterdam, 2001, p. 139.

[48] P. Hamon, L. Toupet, J.-R. Hamon, and C. Lapinte, *Organometallics*, 1992, **11**, 1429.

[49] M. Jiménez-Tenorio, M. C. Puerta, and P. Valerga, *Organometallics*, 1994, **13**, 3330.

[50] B. Pleune, D. Morales, R. Meunier-Prest, P. Richard, E. Collange, J. C. Fettinger, and R. Poli, *J. Am. Chem. Soc.*, 1999, **121**, 2209.

[51] J. N. Harvey and M. Aschi, *Phys. Chem. Chem. Phys.*, 1999, **1**, 5555.

[52] J. C. Green, J. N. Harvey, and R. Poli, *J. Chem. Soc, Dalton Trans.*, 2002, 1861.

[53] M. J. Frisch, G. W. Trucks, H. B. Schlegel, G. E. Scuseria, M. A. Robb, J. R. Cheeseman, V. G. Zakrzewski, J. Montgomery, J. A., R. E. Stratmann, J. C. Burant, S. Dapprich, J. M. Millam, A. D. Daniels, K. N. Kudin, M. C. Strain, O. Farkas, J. Tomasi, V. Barone, M. Cossi, R. Cammi, B. Mennucci, C. Pomelli, C. Adamo, S. Clifford, J. Ochterski, G. A. Petersson, P. Y. Ayala, Q. Cui, K. Morokuma, D. K. Malick, A. D. Rabuck, K. Raghavachari, J. B. Foresman, J. Cioslowski, J. V. Ortiz, A. G. Baboul, B. B. Stefanov, G. Liu, A. Liashenko, P. Piskorz, I. Komaromi, R. Gomperts, R. L. Martin, D. J. Fox, T. Keith, M. A. Al-Laham, C. Y. Peng, A. Nanayakkara, C. Gonzalez, M. Challacombe, P. M. W. Gill, B. Johnson, W. Chen, M. W. Wong, J. L. Andres, C. Gonzalez, M. Head-Gordon, E. S. Replogle, and J. A. Pople, 'Gaussian 98, Revision A.9', Gaussian, Inc., 1998.

[54] A. D. Becke, *J. Chem. Phys.*, 1993, **98**, 5648.

[55] A. Schaefer, H. Horn, and R. Ahlrichs, *J. Chem. Phys.*, 1992, **97**, 2571.

[56] A. J. H. Wachters, *J. Chem. Phys.*, 1970, **52**, 1033.

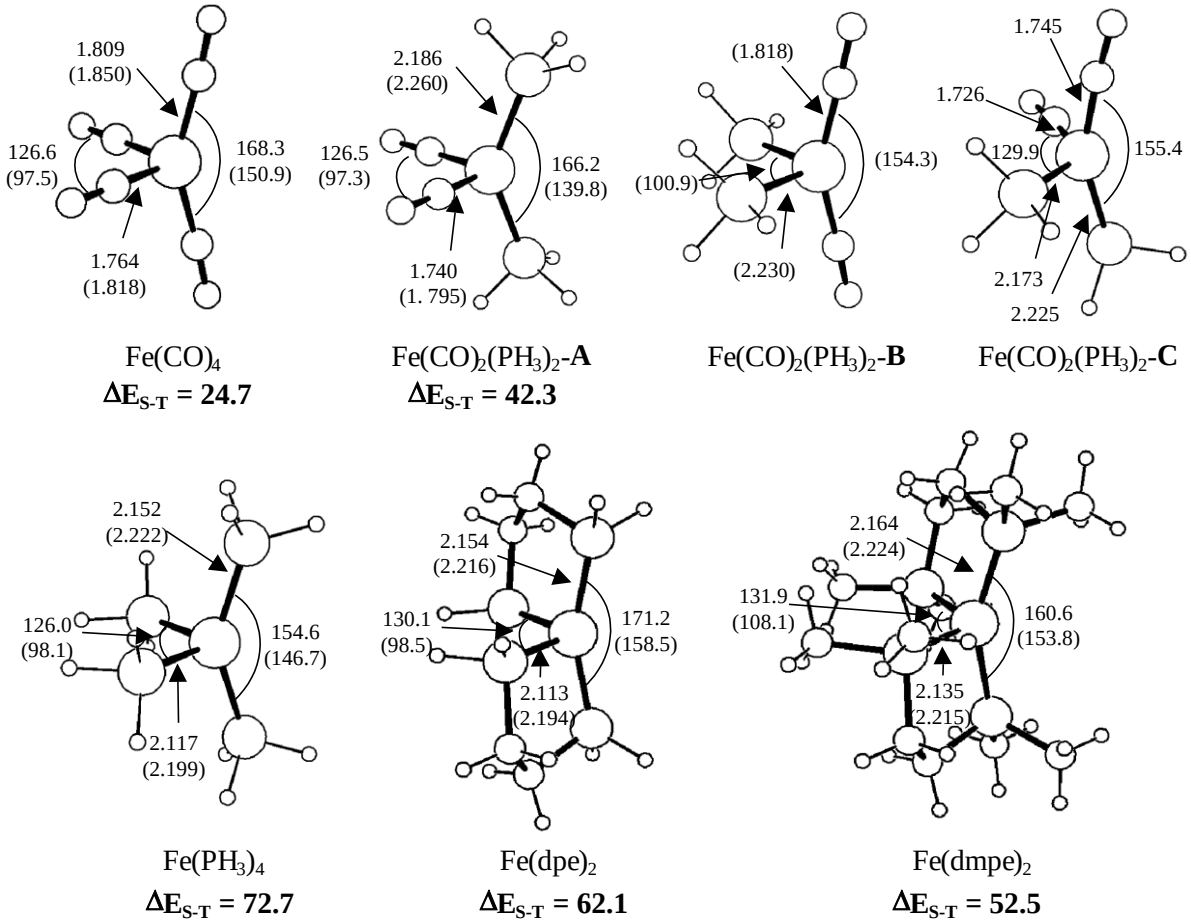

Figure 1. Optimized geometries (distances in Å, angles in degrees; values above are for the singlet, below in parentheses for the triplet) and triplet-singlet gaps (ΔE_{S-T} in kJ mol^{-1}) of the 16-electron Fe(0) systems.

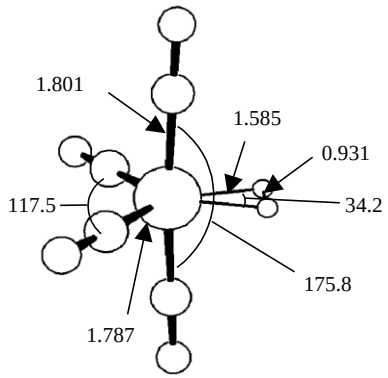

$Fe(CO)_4(H_2)$

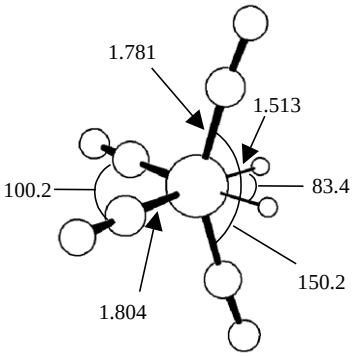

$Fe(CO)_4(H)_2$

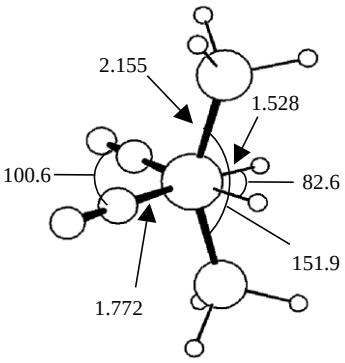

$Fe(c\text{-}CO)_2(t\text{-}PH_3)_2(c\text{-}H)_2$

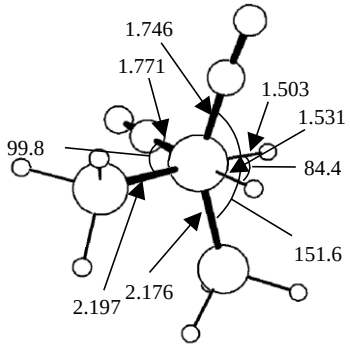

$Fe(c\text{-}CO)_2(c\text{-}PH_3)_2(c\text{-}H)_2$

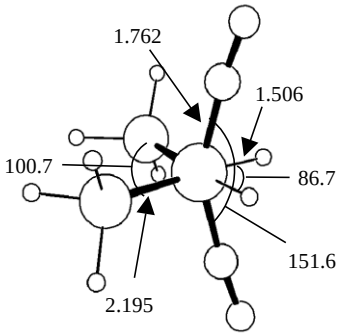

$Fe(t\text{-}CO)_2(c\text{-}PH_3)_2(c\text{-}H)_2$

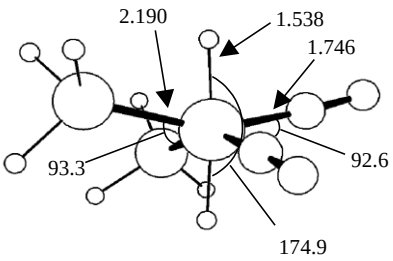

$Fe(c\text{-}CO)_2(c\text{-}PH_3)_2(t\text{-}H)_2$

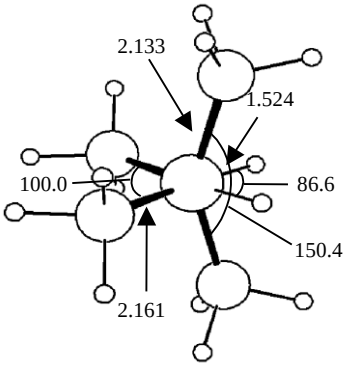

$Fe(PH_3)_4(H)_2$

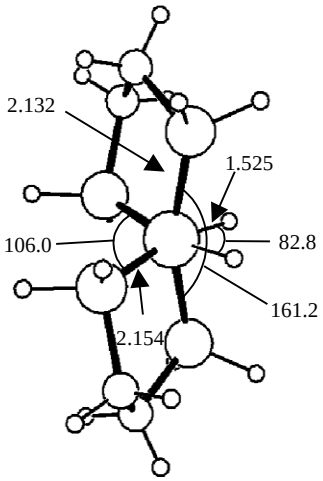

$Fe(dpe)_2(H)_2$

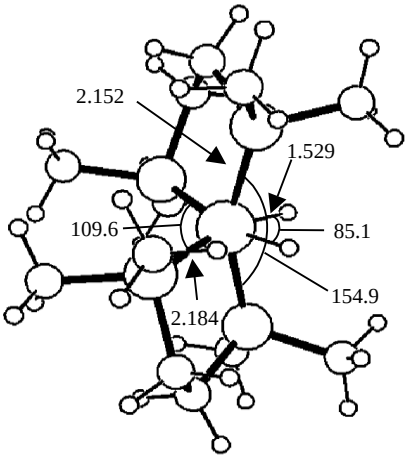

$Fe(dmpe)_2(H)_2$

Figure 2. Optimized geometries (distances in Å, angles in °) of the dihydride products.

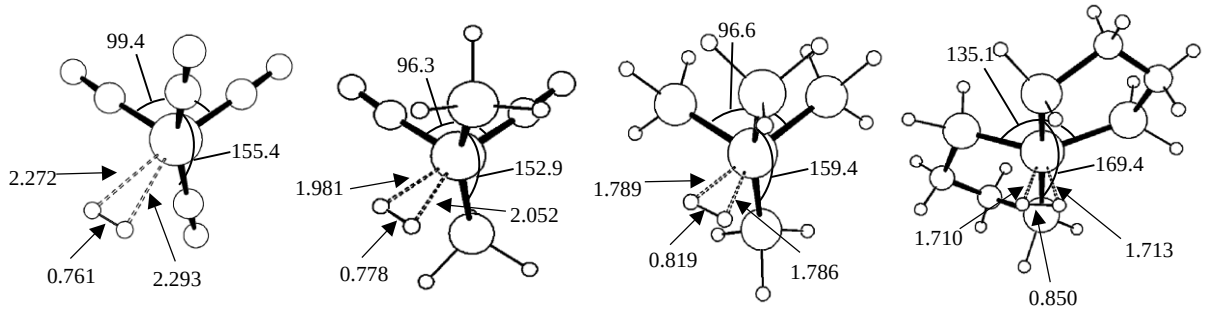

Figure 3. Optimized geometries (distances in Å, angles in degrees) of the MECPs.

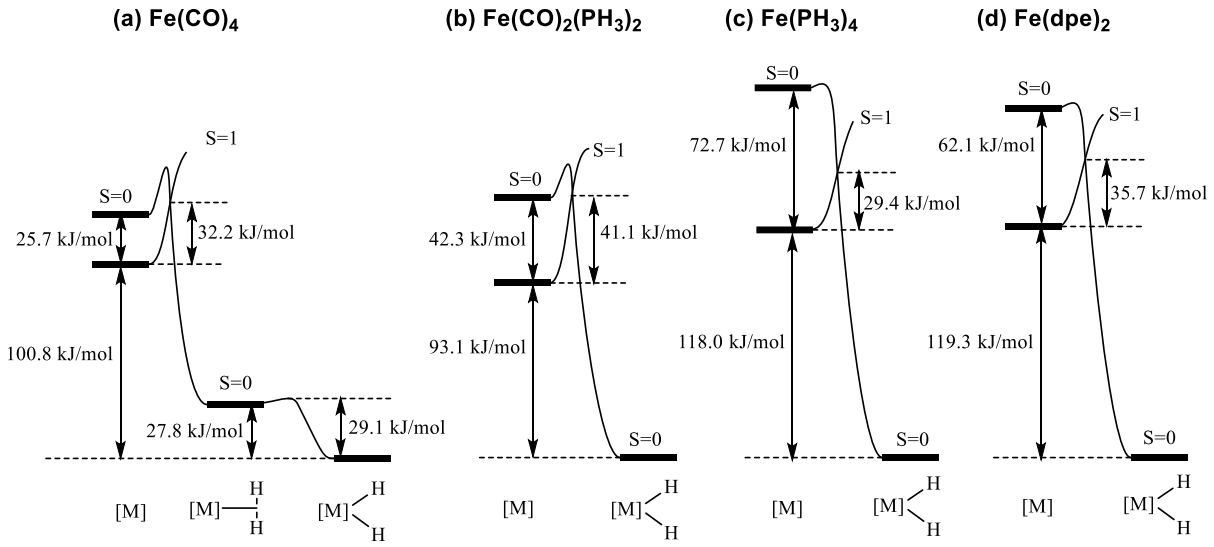

Figure 4. Relative energies of the $FeL_4 + H_2$ systems [FeL_4 = $Fe(CO)_4$ (a); $Fe(CO)_2(PH_3)_2$ (b); $Fe(PH_3)_4$ (c); $Fe(dpe)_2$ (d)], including the MECP.

Table 1. Relative energies for the H_2 addition to 16-electron Fe(0) systems.

	ΔE/kJ mol^{-1}	ΔG/kJ mol^{-1}	ν(Fe-H) sym./cm^{-1}	ν(Fe-H) asym. /cm^{-1}	ν(H-H) /cm^{-1}
$^1Fe(CO)_4 + H_2$	126.52	77.32			
$^3Fe(CO)_4 + H_2$	100.79	45.15			
$^{1/3}Fe(CO)_4 \bullet H_2$	132.97				
$Fe(CO)_4(H_2)$	27.80	27.12	1848.7	995.0	2313.8
TS (C-NC)	29.09	22.42	1989.0	1984.2	(574.9)[a]
$Fe(CO)_4(H)_2$	0.00	0.00	1986.7	1970.0	-
$^1Fe(CO)_2(PH_3)_2$-**A** + H_2	136.22	84.97			
$^1Fe(CO)_2(PH_3)_2$-**C** + H_2	151.80	95.53			
$^3Fe(CO)_2(PH_3)_2$-**A** + H_2	93.91	33.41			
$^3Fe(CO)_2(PH_3)_2$-**B** + H_2	118.25	58.34			
$^{1/3}Fe(CO)_2(PH_3)_2$-**A**$\bullet H_2$	135.00				
$Fe(c\text{-}CO)_2(t\text{-}PH_3)_2(c\text{-}H)_2$	0.00	0.00	1922.9	1900.3	
$Fe(c\text{-}CO)_2(c\text{-}PH_3)_2(c\text{-}H)_2$	3.50	2.08	1978.0[b]	1905.6[c]	-
$Fe(t\text{-}CO)_2(c\text{-}PH_3)_2(c\text{-}H)_2$	6.70	3.84	1974.0	1965.0	-
$Fe(c\text{-}CO)_2(c\text{-}PH_3)_2(t\text{-}H)_2$	37.25	36.20	1934.0	1796.4	-
$^1Fe(PH_3)_4 + H_2$	191.57	128.78			
$^3Fe(PH_3)_4 + H_2$	118.91	58.78			
$^{1/3}Fe(PH_3)_4 \bullet H_2$	148.31				
$Fe(PH_3)_4(H)_2$	0.00	0.00	1890.8	1879.0	-
$^1Fe(dpe)_2 + H_2$	181.41	128.43			
$^3Fe(dpe)_2 + H_2$	119.34	62.67			
$^{1/3}Fe(dpe)_2 \bullet H_2$	154.98				
$Fe(dpe)_2(H)_2$	0.00	0.00	1889.1	1876.4	-
$^1Fe(dmpe)_2 + H_2$	190.75	139.05			
$^3Fe(dmpe)_2 + H_2$	138.25	77.18			
$Fe(dmpe)_2(H)_2$	0.00	0.00	1874.3	1859.6	-

[a]Imaginary frequency. [b]Mostly *trans* to PH_3. [c]Mostly *trans* to CO.

Synopsis

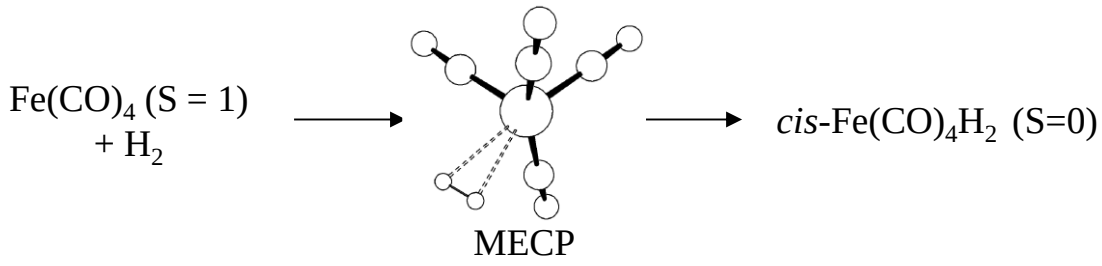

The oxidative addition of H_2 to the spin triplet 16-electron Fe(0) complexes $Fe(CO)_4$, $Fe(CO)_2(PH_3)_2$, $Fe(PH_3)_4$, $Fe(H_2PCH_2CH_2PH_2)_2$ and $Fe(Me_2PCH_2CH_2PMe_2)_2$ has been investigated by DFT methods, including the explicit location of the minimum energy crossing point (MECP).